

Original papers

RetIS: Unique Identification System of Goats through Retinal Analysis



Subhranil Mustafi*, Pritam Ghosh, Satyendra Nath Mandal

Department of Information Technology, Kalyani Government Engineering College, Kalyani 741235, India

ARTICLE INFO

Keywords:

Goat fundus imaging
Biometric authentication
Active contouring
Hamming distance
Retinal recognition

ABSTRACT

Developing an accurate, reliable and tamper-proof unique identification system for identifying individual animals is one of the most important but challenging tasks in intelligent livestock management. Currently, unique identification for animals is done using methods like stenciling, ear tagging, ear notching, branding, etc. which create opportunities for the poachers, middle men and animal thieves to manipulate the tags and transfer animals across international borders, claim false insurance, poach for their meat, bones, etc. illegally. This becomes a huge headache for the livestock owners. In this paper, a novel biometric unique identification system called "RetIS" has been developed based on goat retinal image which is unique, tamper-proof, reliable and accurate. The identification system has been developed based on the origination and distribution pattern of the blood vessels through a circular ring around the optic disc, which remains constant for the entire lifetime of the goat. Goat retinal images have been captured using a handheld fundus camera. The captured images are then segmented, normalized and encoded for the creation of templates, which are eventually stored in a database for matching with query templates based on hamming distance criteria. In matching, it has been observed that if the hamming distance between stored and query template is less than equal to 0.37 (matching $\geq 63\%$), it can be confirmed that the stored and query template belongs to the same individual goat providing its unique identification, otherwise the templates belong to two separate individual goats. This model has been tested with more than 200 retinal images obtained from twelve different goats producing 99% accuracy. The performance of this proposed model has been compared with other animal identification technologies and is found to be the most accurate and precise.

1. Introduction

As per the Livestock Census of 2019, India has a huge goat population of around 148.8 million. All these goats are identified either by Stenciling, Branding, etc. or by attaching RFID tags around the neck collar which can easily be manipulated (Roy et al., 2021). The lack of a unique, non-invasive and reliable identification system (Mustafi et al., 2021; Mustafi et al., 2020) creates opportunities for poachers, middle men and animal thieves to manipulate tags and transfer animals across international borders, poach for their meat, bones, etc. illegally.

The solution to such problem is the use of distinctive behavioral and biological characteristics of an individual which is termed as biometrics (Shaydyuk and Cleland, 2016). This emerging technology takes unique patterns and features from the body itself to facilitate automatic recognition and identification of technologies. Behavioral biometrics analyses certain behavior of any individual such as voice, behavior within the herd, etc. while morphological biometrics analyses vein,

muzzle, tail pattern, iris, retina, etc. Of these, the iris and retina of the eye provide the most authentic mode of physiological biometric identification. Due to the stability and time-efficient feasibility, identification through iris pattern gathered generous interest in commercial viability of the product (Zhu et al., 2000). Although, the process of acquiring images for retinal analysis is not time-efficient, but the uniqueness in the vascular patterns of the retinal images makes it nearly impossible to forge contrary to that of iris.

The uniqueness of the retinal vascular pattern for every individual based (used for authentication) (Deljavan Amiri et al., 2009; Fukuta et al., 2008; Singh et al., 2016) had been established and later published in a research paper by Drs. Carleton and Goldstein during the study of eye diseases (Bevilacqua et al., 2008). Later, it had been supported by Dr. Tower in the course of studying two identical twins wherein amidst of most likely physiological factors, the retinal vascular pattern had been found completely different in one another (TOWER, 1955).

Such established technology for humans (Chihaoui et al., 2015,

* Corresponding author.

E-mail addresses: suhhranilmustafi2011@gmail.com (S. Mustafi), ghoshpritam25@gmail.com (P. Ghosh), satyen_kgec@rediffmail.com (S.N. Mandal).

2016; Ortega et al., 2006) had been tried to be incorporated in goats, but due to the heterogenous color intensity of the background and arbitrary size of blood vessels in goats (Bhayani and Vyas, 2014), it had been found difficult to generate any specific information out of such image. Helping the livestock population of goats by developing a unique, reliable and non-invasive identification system against all such odds motivated us to overcome the research gap and pursue this research work.

The aim of this paper is to propose a novel identification system of goats through retinal image analysis by taking a uniform circular ring as a metric for generation of templates and matching between them. The novel identification algorithm "RetIS", consists of image acquisition step to capture pictures of retina using Volk-inView fundus camera (USER'S MANUAL/INSTRUCTIONS FOR USE Volk INview Retinal Camera, n.d.) along with iPhone 6. Also, to restrain the goat in a fixed position safely, a goat restraining tool has been developed (Patent Application No. 201831033038) and implemented for image acquisition. After acquiring images, the vascular pattern in the ring is enhanced using contrast stretching (Rubini and Pavithra, 2019) by using Contrast Limited Adaptive Histogram Equalization Process (CLAHE) (Liu et al., 2019; Setiawan et al., 2013). After localizing the optic disc using the active contour model, outer mask is generated having radial dimension of 100 pixels and centering along the centroid of the optic disc. The final mask is then applied over the initial contrast enhanced image to get the segmented image. Image Normalization is then performed over the segmented image into a rectangular image having length of 240 pixels and breadth of 20 pixels, with the help of Daugman's rubber sheet model (Johar and Kaushik, 2015). Linear interpolation has been used to extract the intensity values into the normalized polar coordinates resulting in the generation of the polar array.

The normalized two-dimensional pattern is then encoded using the Log-Gabor wavelets and resulted in the generation of biometric templates. Eventually, these biometric templates are used for matching between same and different individuals using the concept of hamming distance (Atallah and Duket, 2011).

Contributions through this paper are as follows:

- This paper proposes the novel identification technology for individual goat identification and recognition using retinal image analysis overcoming all odds favouring the heterogenous colour intensity of the background & arbitrary blood vessels of the goat retina image.
- An innovative approach has been applied to capture retinal pictures for non-obedient or non-communicative animals.
- A new database consisting of Goat Fundus Images and their corresponding templates have been created.

The following paper is broadly divided into 8 sections. Starting with introduction in Section 1, followed by difference between human and goat retina in Section 1.1, the related works is discussed in Section 2. The proposed methodology is discussed in Section 3, having Image Acquisition in Section 3.1, Image Pre-Processing & Selection in Section 3.2, Enhancement in Section 3.3, Image Segmentation in Section 3.4, Normalization in Section 3.5, Feature encoding in Section 3.6, Matching in Section 3.7, Results & Discussions in Section 4, results of same goat in Section 4.1 and for different goat in Section 4.2, performance evaluation of the algorithm in Section 5, Performance Comparison in Section 6 followed by database description in Section 7 & conclusion in Section 8.

1.1. Human retina vs. goat retina

The human identification algorithms based on retinal images are not applicable in goat identification due to anatomical differences of retinal structure. The presence of rods and cones cells help in visualizing in dim-lit and well-lit conditions. The human retina has a well-defined optic disc, which can easily be located, blood vessels and a homogenous colour intensity of the background, while the presence of extra cone cells lead to the generation of heterogenous colour intensity of the

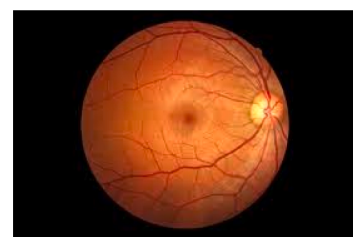


Fig. 1a. Human Retina.

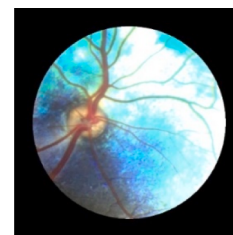


Fig. 1b. Goat Retina.

background and arbitrary thickness of blood vessels while moving away from the optic disc leads to the failure of incorporating the established human identification system through retina (Fraz et al., 2012; Fukuta et al., 2008) in goats (Figs. 1a and 1b).

2. Related works

Köse and Ikibaş (2011) stated that the retinal vasculature in fundus images can be used to authenticate any individual and such system's supremacy lies in toleration against alteration & scale invariance. Gonzales Barron et al. (2008) stated that the lighting conditions cannot modulate the matching-score values of the built-in algorithm but the light reflex phenomenon in pupils played a major role in lowering the matching score values taken outdoors. The contrast enhancement using CLAHE can be used to acquire a better accuracy during the matching as stated by Setiawan et al. (2013). Shaydyuk and Cleland (2016) explained that liveness detection must be incorporated to make the acquisition system less susceptible to deception and that can be achieved by retinal scanning. Muhammed (2018) stated that the optic disc should be localized first as it marks the origin of the blood vessels and also contain the distribution pattern. Elangovan and Nath (2019) stated that unique features in retina can be both vascular and non-vascular patterns, but vascular patterns are the most prominently used by researchers in pursuing template generation & unique identification. S.L. et al. (2017) found out that the average thickness of retina is about 100–500 µm and the retinal patterns in animal does not change for up to 6 h after its death. Rusk et al. (2006) claimed that retinal identification system is a viable method for Beef & Sheep identification and recognition as it provides as accuracy of 98.6% and 84.9% against nose prints showing accuracy of 68.9% and 79.5%. After researching in cattle identification (Small, 2015), claimed that the vascular pattern of retina does not change with the passing of age. Apart from uniqueness and performance, circumvention is an important parameter which help in measuring the reliability of the system and how easily the system can be be-fooled by the fraudulent methods and techniques (De Luis-García et al., 2003; Maltoni et al., 2009; Unar et al., 2014). Nicholas Millichamp, B.V.Sc, Ph.D said that some variations in iris pigmentation can be seen over time obtained by infrared light but more evidence of vascular changes could be obtained in a normal light photograph in case of pigmentation, quoted by Kane (2011). Rani and Rani (2017) surveyed and concluded that the K-Nearest Neighbour Random Forest Classifier along with Histogram Equalization can be used to improve the accuracy of

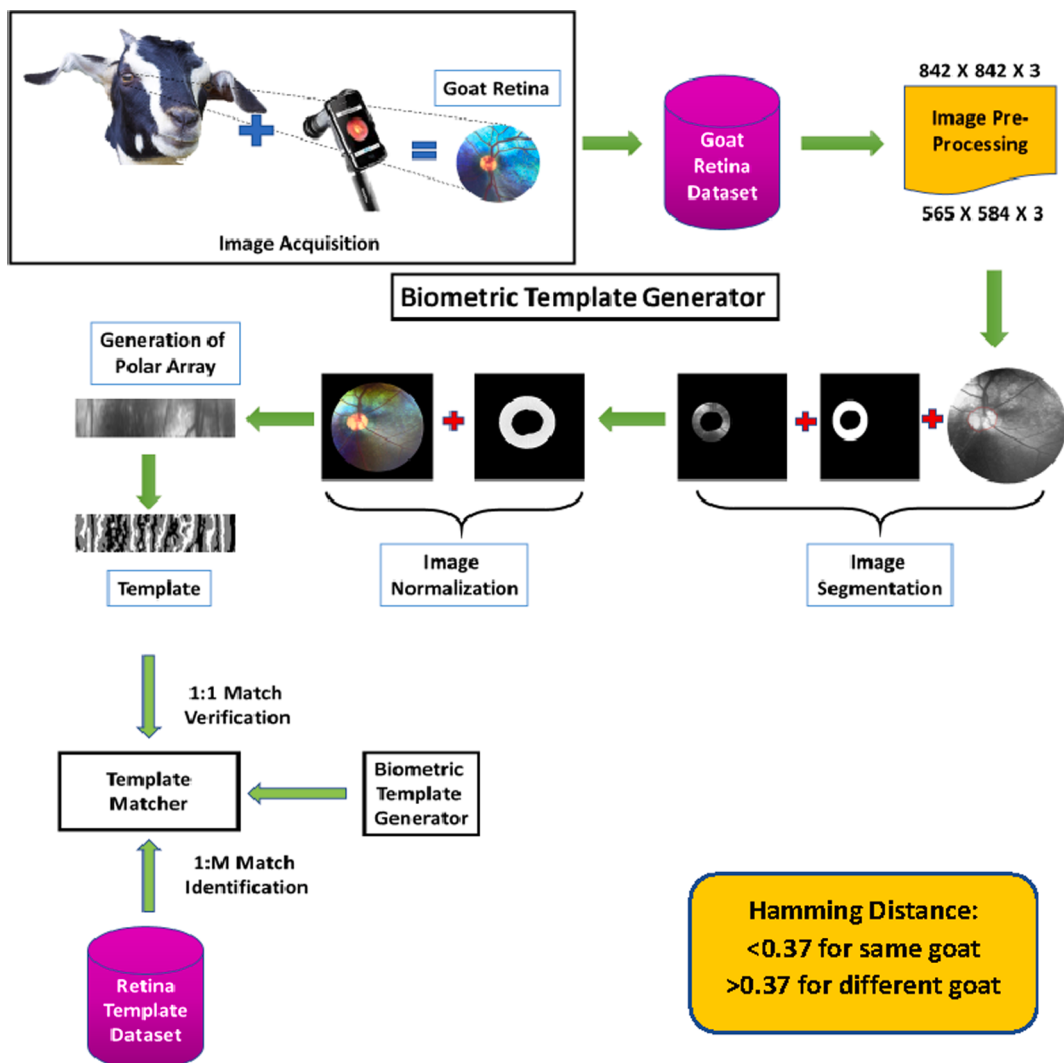


Fig. 2. The Proposed algorithm of 'RetIS'.

Table 1
Camera specifications for image acquisition standards.

iPhone 6	
Display Resolution:	750 X 1334 Pixels
Camera	
Megapixels	8 MP
Aperture	f/2.2
Sensor Size	1.5 micron
Volk-inView Camera	
Power Source	Internal Electronic Camera device battery
Working Distance	50mm
Angle of View	50°/80°
Light Source	LED
Digital Resolution	918 X 918 Pixels

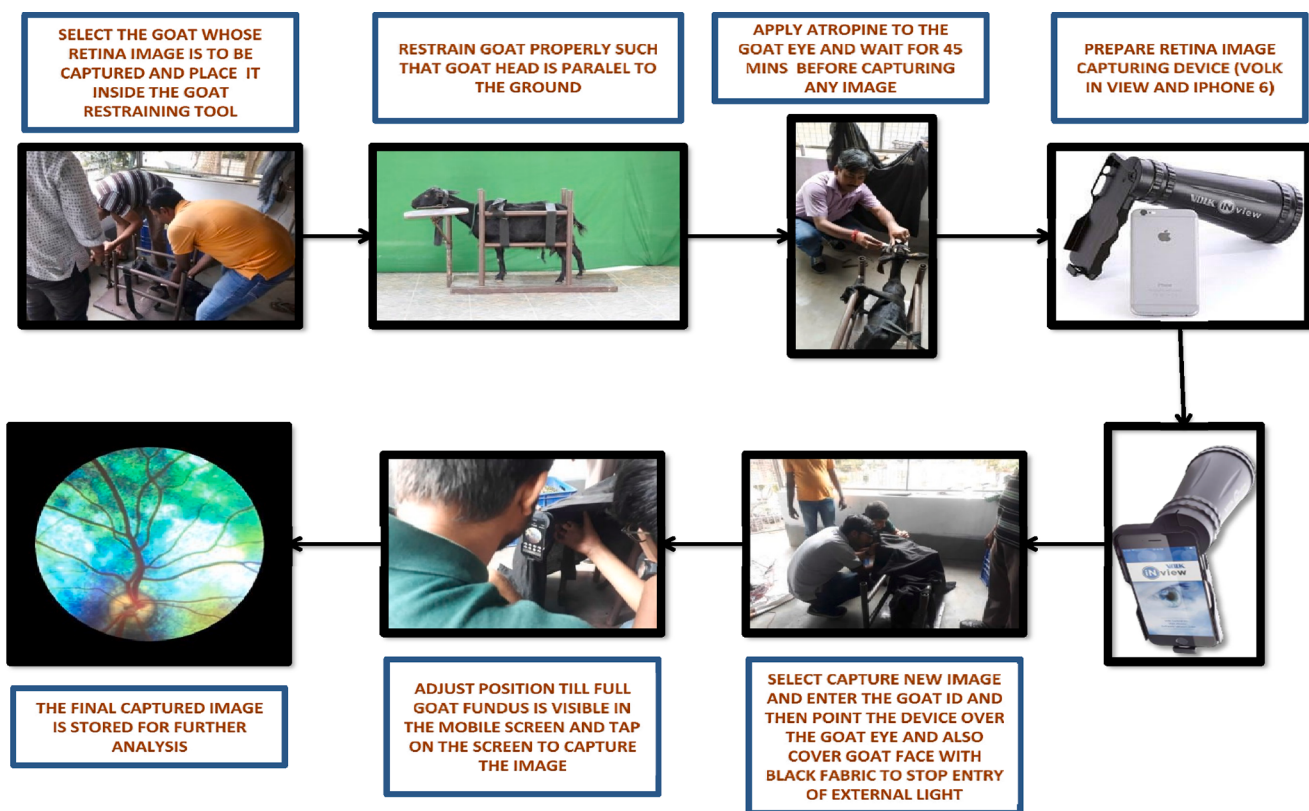


Fig. 3. Image Acquisition of Goat Retina.

classification especially in case of humans on biometric retinal images.

3. Proposed methodology of “RetIS”

The algorithm of “RetIS” have the following steps necessary for generation of unique identification in the form of templates and matching between same and different templates to calculate the threshold have been shown in Fig. 2:

The steps associated with the proposed methodology, “RetIS” has been discussed accordingly:

- 3.1. Retinal Image Acquisition
- 3.2. Pre-Processing & Selection of Images
- 3.3. Image Enhancement through Contrast Stretching

3.4. Image Segmentation

3.5. Image Normalization

3.6. Feature Encoding and Template Generation

3.7. Matching with same or different templates.

3.1. Retinal image acquisition

This is the initial step for the unique goat identification process. The retina of the goat has been captured by using the Volk-inView fundus camera with iPhone 6 in a controlled environment.

An innovative method pertaining to the capture of the fundus image for non-obedient & non-communicative animals has been devised with the help of the Goat Restraining Tool (*discussed in Section 4.2*).

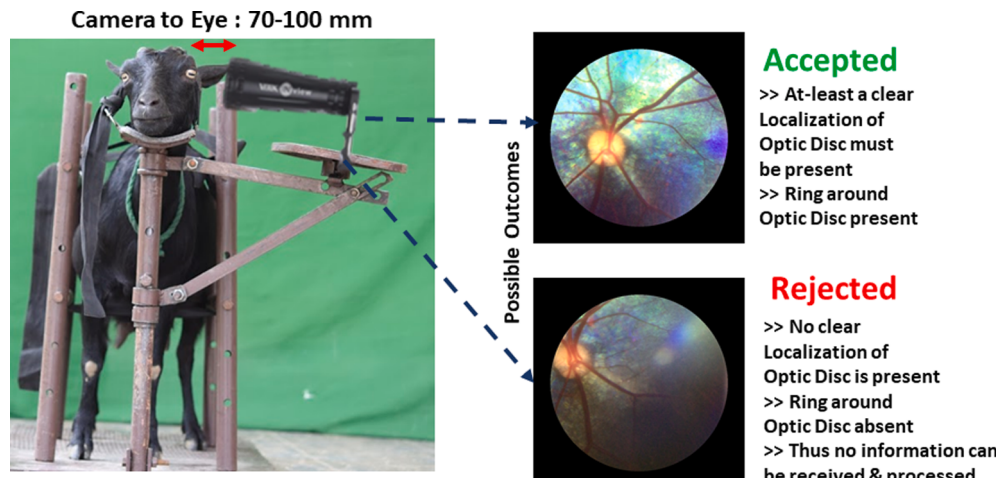


Fig. 4. Image Acquisition Standards for “RetIS”.

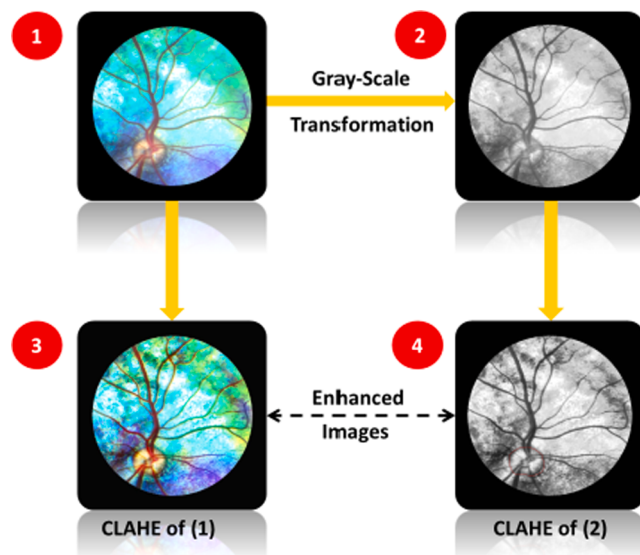


Fig. 5. Image Enhancement.

Exhaustive synthesis related to digital fundus cameras and their technological advances is discussed in [Bernardes et al. \(2011\)](#), [Panwar et al. \(2016\)](#) and [Zhi et al. \(2012\)](#). Atropine solution has been applied to dilate ([Atropine Sulfate Drops, n.d.](#)) the pupil for 40–45 min so that clear image of the retina can be taken using the fundus camera. The dedicated mobile application and the camera having lens of power 20 dioptre has been used to take images of goat retina. The Volk-inView fundus camera has a visualization of 50° field ([The Finest Ophthalmic Imaging Catalog, 2019](#)), which is the portion of the object that fills the camera's sensor ([Kachouri et al., 2020](#)). The specifications of iPhone 6 and Volk-inView Fundus camera is described in [Table 1](#).

The flow chart for image acquisition of Goat Retina using Volk-inView Camera attached with iPhone 6 is shown in [Fig. 3](#).

3.2. Pre-processing & selection of images

Several factors have been coordinated during the image acquisition process to generate the best results during template generation and pattern matching, such as camera-to-eye distance, level of illumination of the eye and the amount reflection from the eye. Later it has been resized in 565 × 584. Not only instrument, but also there are certain image acquisition standards which have been adhered to get a near to perfect noise free image. The acceptance of the image based on the image acquisition standards, is then sent for further processing by “RetIS”. The database, “GoatRetDB-KGEC” has been created based on

the retina images collected from Indian Veterinary Research Institute (IVRI), Kalyani, West Bengal. Such image acquisition standard is depicted in [Fig. 4](#).

3.3. Image enhancement

To distinguish between the vascular patterns and optical disc inside the retina from the heterogenous background, Contrast Limited Adaptive Histogram Equalization (CLAHE) has been used to improve the contrast of the images ([Setiawan et al., 2013](#)). The adaptive histogram helps in computing several histograms pertaining to each section of the image which is distinct and uses such values to redistribute the values of lightness in the image. The suitability of the technique lies in the fact that the local contrast and the edges can be enhanced in each region of the image. And the contrast is changed according to the average values of the contrast of the neighbourhood pixels to the specific location. The distinction between the ordinary image and adaptive contrast enhanced image is depicted in [Fig. 5](#).

3.3.1. Contrast Limited adaptive histogram Equalization (CLAHE)

CLAHE is governed by two parameters: Block Size (BS) and Clip Limit (CL)

The original histogram is clipped and such clipped pixels are thereby redistributed to each grey level. The complete image is distributed into 8×8 tiles and cumulative distribution function has been calculated on each tile. Pixels in blue are bilinearly interpolated, pixels in green are linearly interpolated and pixels in the corners are transformed according to the transformation function, leading to the generation of the CDF for each tile ([Fig. 6](#)). Separating the RGB colour space into R, G & B, they are enhanced by the Rayleigh Transformation function (Eq. (1)) (which depends on the average number of pixels governed by the clip limit and block size which flattens the histogram and increases the range dynamically respectively) and recombined to produce the final result.

$$y(i) = y_{min} + \sqrt{2\alpha^2 \ln\left(\frac{1}{1 - P_{input}(i)}\right)} \quad (1)$$

where y_{min} is the lower bound of the pixel value and α is the scaling parameter which depends on the input image.

The output probability density function for each intensity value is given by Eq. (2):

$$p(y(i)) = \frac{(y_i - y_{min})}{\alpha^2} \cdot \exp\left(-\frac{(y_i - y_{min})^2}{2\alpha^2}\right) \text{ for } y(i) \geq y_{min} \quad (2)$$

where an increase in α will result in more contrast enhancement, leading to increase in saturation value along with the amplification of noise levels.

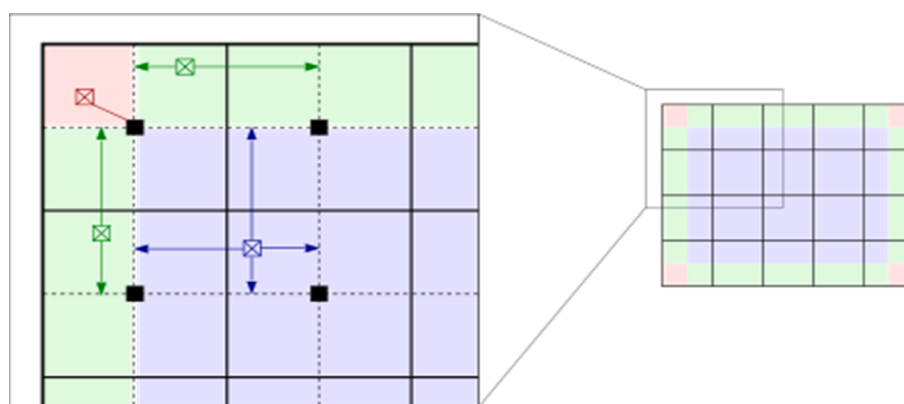


Fig. 6. Pictorial Representation of CLAHE (Source: Wikipedia).

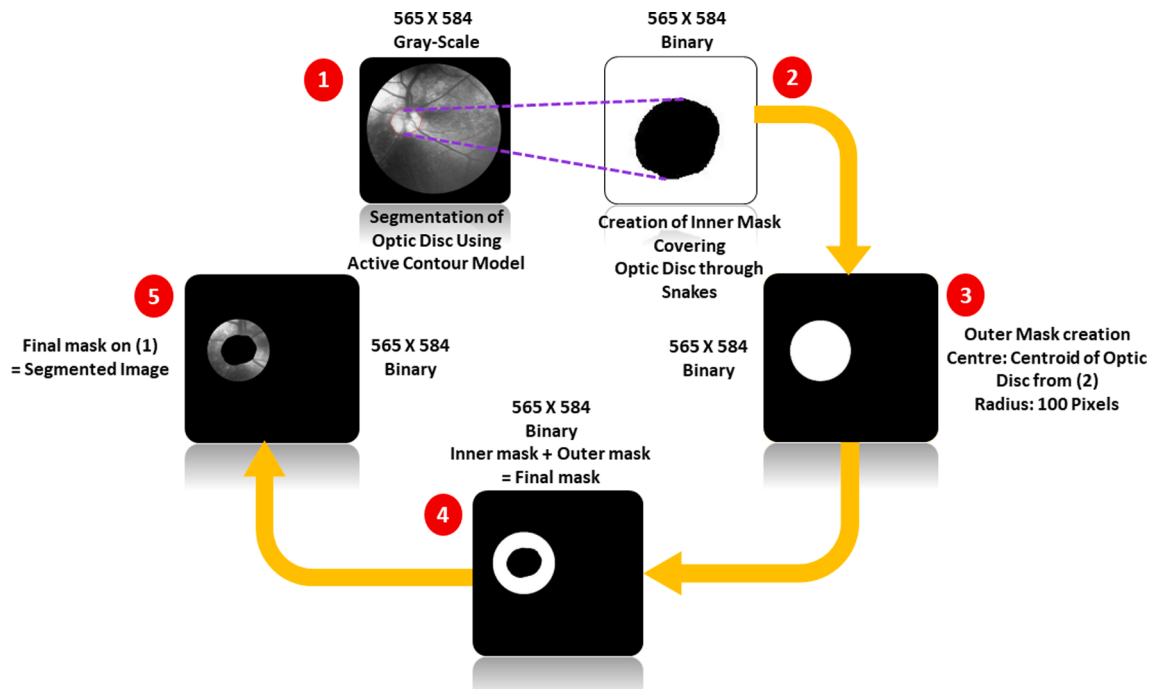


Fig. 7. Steps pertaining to Image Segmentation.

3.4. Image segmentation

The image has been segmented by tracing out the optic disc using the active snake contour algorithm which is an energy minimising spline curve influenced by image forces and guided by the externally applicable constraint forces which pull it towards certain features of the curve such as lines and the edges. Snakes help in locking onto the nearby edges thus help in localizing them accurately. After selecting few points manually, the contour tracing algorithm has been able to develop a closed curve based on such starting and terminating pixels and expanding or contracting the curve based on the change in the energy of the intensity levels of each pixel, thereby creating a binary mask having '0' intensity values inside and '1' intensity values outside the curve. Interacting with such models help us in exploring the energy landscape easily and generating effective energy functions that have a few local minima and least dependence on the starting points. They are called snakes due to the ability to minimize the energy functional and exhibition of the dynamic behaviour.

The *controlled continuity spline* is the basic snake model influenced by the external constraint and image forces. The piecewise smoothness constraint is imposed by the internal spline forces and the image forces push the snake in the direction of the salient features such as edges, lines and subjective contours. Putting the snake near the desired local minimum is pertained by the external constraint force.

Representing the position of the snake parametrically by $v(s) = (x(s), y(s))$, the energy functional can be depicted in Eq. as,

$$E_{\text{snake}}^* = \int_0^1 E_{\text{snake}}(v(s)) ds \quad (3)$$

$$= \int_0^1 E_{\text{int}}(v(s)) + E_{\text{image}}(v(s)) + E_{\text{con}}\left(v(s)\right) ds$$

where the internal energy of the spline due to bending is denoted by E_{int} , E_{image} is the energy due to image forces and E_{con} depicts the energy due to external constraint forces. E_{int} can be depicted in Eq. (4).

$$E_{\text{int}} = (\alpha(s)|v_s(S)|^2 + \beta(s)|v_{ss}(S)|^2)/2 \quad (4)$$

The first-order term is controlled by $\alpha(s)$ and second-order term is

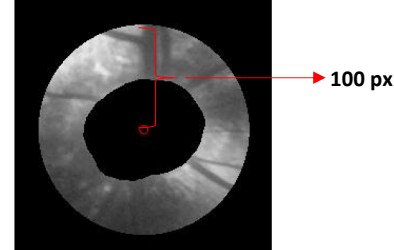


Fig. 8. Analysis of Vascular pattern through a ring around Optic Disc.

controlled by $\beta(s)$. The complete steps for image segmentation have been depicted in Fig. 7.

Merits & applications regarding usage of a circular ring around the optic disc as a parameter to develop unique identification template for each individual is discussed in Section 3.4.1.

3.4.1. Using a ring around the optic disc as a metric

The vascular pattern around the optic disc is used to generate template for each individual goat, through the ring extracted after the image segmentation process. The vascular pattern information visible through the ring are more important as they contain rich density of information and are less noisy. On the other hand, as they move farther from the optic disc, the distribution pattern becomes thinner and arbitrary. Hence, choosing a region around the optic disc proves to be efficient (*observed from the results section*) as the vascular patterns are distinct, prominent and have thicker vessels (Fig. 8).

3.5. Image Normalization

After extracting the ring having a high density of blood vessel pattern information, it has been transformed into fixed dimensions. The purpose of normalization is to achieve shift and scale invariance. A geometric method has been used here for goat retina normalization. The centroid of optic disc has been considered as the reference point, and the radial vector passes through it (as shown in Fig. 9(1)). A constant number of

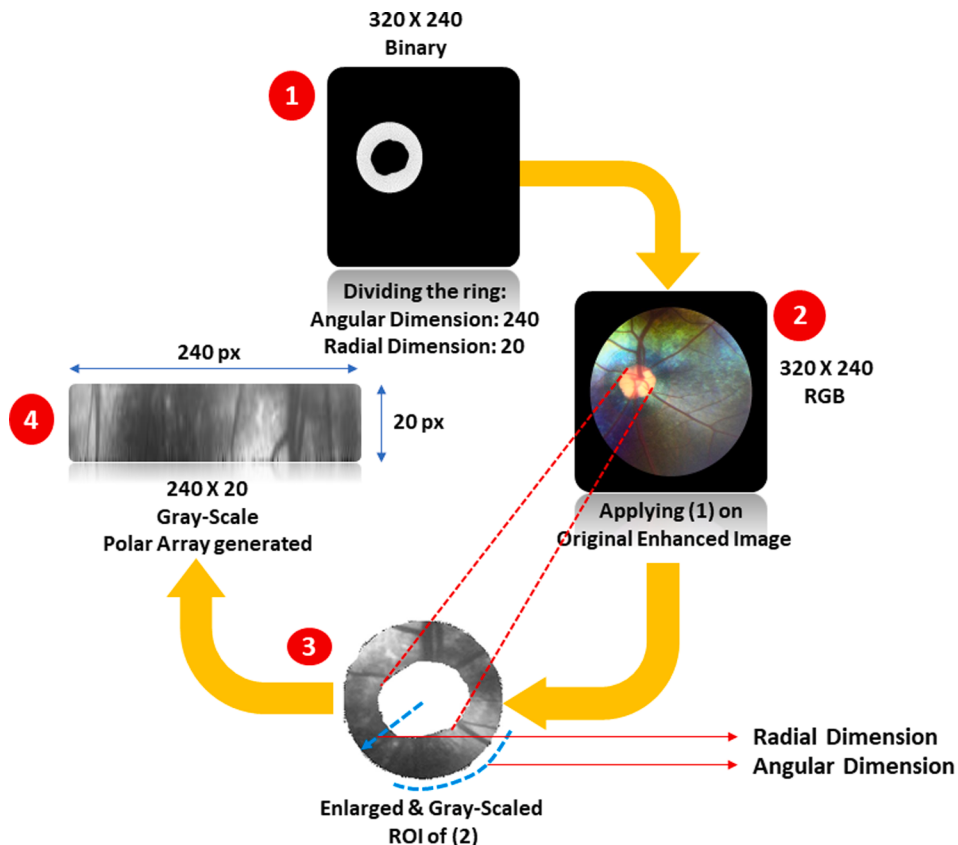


Fig. 9. Steps pertaining to Image Normalization.

points have been chosen along each radial line so that a constant number of radial data points are taken from the ring around the optic disc of the retina. The radial and angular position in the normalized pattern eased in finding out the cartesian coordinates of the data points by backtracking. In this experiment, we have taken the radial resolution 20 and angular resolution 240. So, the dimension of the normalized image is $240\text{px} \times 20\text{px}$, 8bit grayscale image. Intensity values into the normalized polar representation have been extracted based on the linear interpolation method. Steps have been shown in Fig. 9.

Fig. 9(3) has been gray-scaled and extracted from Fig. 9(2) after applying Fig. 9(1) on the enhanced original RGB image of the retina. To denoise the intensity values of the region of interest (ROI), the values of

neighbouring pixels have been aggregated and interpolated to generate the polar array as shown in Fig. 9(4). This polar array, after passing through convolution using 1D Log Gabor wavelets and corresponding values being phase quantised, eventually lead to the generation of templates having information stored in the form of matrix.

The intensity of each coordinate in Fig. 9 has been arranged in the form of a rectangular block preserving the integrity of the coordinates with respect to its neighbours and thus rectangular polar array is generated with a fixed size $W \times H$ i.e., 240×20 pixels.

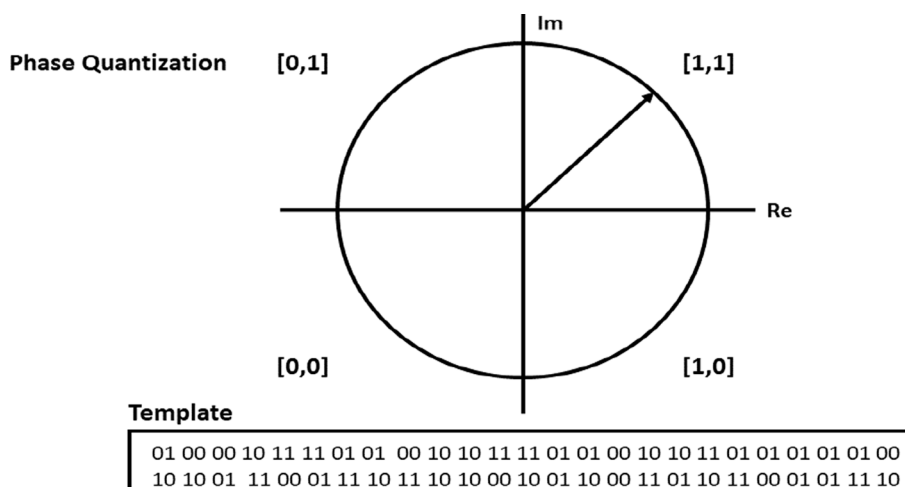
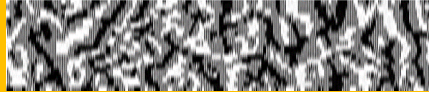


Fig. 10. Template Generation and Phase Quantization.

Table 2

Image encoding & biometric template generation.

Biometric Template	Description
	This biometric template is generated from the polar array using the log-Gabor wavelet method. Image Size: 240 X 20

3.6. Feature encoding & template generation

Feature encoding has been implemented by convolving the normalised vascular pattern in the ring around the optic disc with 1D Log Gabor wavelets, as proposed by Field (Nava et al., 2012). It has also been suggested that the natural images are coded better, which has Gaussian transfer functions, by using this filter, when viewed by the logarithmic frequency scale. The transfer function of Log-Gabor filter (Pradeep Kumar, 2014) on the scale of frequency is given in Eq. (5).

$$G(f) = \exp\left\{-0.5 * \log\left(\frac{f}{f_0}\right)^2 / \log\left(\frac{\sigma}{f_0}\right)^2\right\} \quad (5)$$

where the centre frequency of the filter is denoted by f_0 , and the bandwidth of the filter by σ .

The 2D normalised vascular pattern has been split into a number of 1D signals and have been performed convolution with 1D Gabor wavelets. Taking the rows of the 2D normalised pattern as 1D signals, each of the rows correspond to the equal radial distance of the normalised ring of vascular pattern. The columns of the normalized pattern are formed by the angular distance, since maximum independence occurs in angular direction (Fig. 10).

The values of the intensity in the noisy areas in the normalized pattern is set as the average value of the intensities throughout the surrounding region, to eliminate or minimize the noise during the output of filtering. Quantizing the output of the filtering through phase to four levels using Daugman's method (Chawla and Oberoi, 2011), two bits of data with each filter for each phasor is achieved. Such output of the phase quantization is depicted in the form of gray code to enable the change in 1-bit only with the passing of quadrants as depicted in Eq. (6) and Fig. 10. This will help in minimizing the disagreeing number of bits, effectively leading to more accuracy in recognition.

$$P(r, \theta) = \tan^{-1}\left(\frac{ImI_p(r, \theta)}{ReI_p(r, \theta)}\right)$$

$$I_p(r, \theta) = \begin{cases} (1, 1) & \text{if } 0^\circ < P(r, \theta) \leq 90^\circ \\ (0, 1) & \text{if } 90^\circ < P(r, \theta) \leq 180^\circ \\ (0, 0) & \text{if } 180^\circ < P(r, \theta) \leq 270^\circ \\ (1, 0) & \text{if } 270^\circ < P(r, \theta) \leq 360^\circ \end{cases} \quad (6)$$

A bit wise template containing number of bits of information has been generated (Table 2) through the encoding process along with a noise mask corresponding to the corrupted areas to mark the bits in the template as corrupt. The regions are also marked in the noise mask where the amplitude is zero, since the phase information would be meaningless at such places. The total number of bits in the template would be the multiplication of the angular resolution and the radial dimension, where the filters are used two times.

3.7. Matching

Since the bit wise comparisons are necessary, the concept of hamming distance (Atallah and Duket, 2011) has been used as a metric for matching of the biometric templates and this algorithm also incorporates noise masking such that only significant bits are only used. The hamming distance (Atallah and Duket, 2011) will be calculated

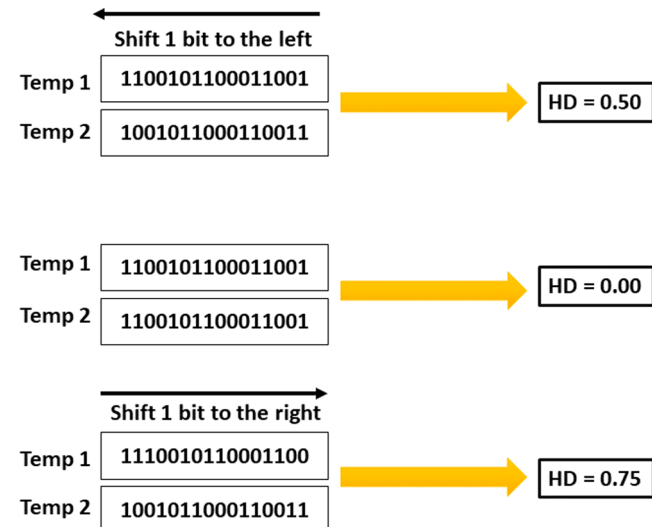


Fig. 11. Examples of Hamming Distance calculation.

based on only the bits of the true vascular pattern region in the ring using the formula in Eq. (7).

$$HD = \frac{1}{N - \sum_{k=1}^N X_{n_k} (OR) Y_{n_k}} \sum_{j=1}^N X_j (XOR) Y_j (AND) X'_{n_j} (AND) Y'_{n_j} \quad (7)$$

where X_j and Y_j denotes two bit wise templates, X'_{n_j} and Y'_{n_j} denotes the noise masks for the corresponding templates and N is the number of bits in each template.

As we come across the theory, the hamming distance (Atallah and Duket, 2011) between two identical vascular patterns would pertain to a value of 0.0 but in practical this does not happen since the normalization is not completely identical and perfect for two identical images of the same retina. Also, effects of noise may differ during the generation of the templates leading to a minimal difference in the matching of intra class retinal vascular patterns inside the ring around the optic disc.

To prevent any rotational inconsistencies, one of the templates is shifted left and right bit-wise and hamming distance (Atallah and Duket, 2011) is calculated at every successive shifts. The horizontal bit wise shifting pertains to rotation of the original vascular pattern inside the ring through the angle given by angular resolution used. If angular resolution used is 240, each shift will pertain to a rotation of around 2° in each shift of the vascular pattern distribution region in the ring. Daugman (Chawla and Oberoi, 2011) suggested this method and helps in correcting the misalignments in the normalized pattern caused due to the rotational differences during imaging. The lowest of all the calculated hamming distance (Atallah and Duket, 2011) values are taken as it pertains to the best match between two templates.

The number of bits shifted has been calculated as twice the number of filters used as each filter generates two bits of information for each pixels of the normalized vascular pattern of the retina. To normalize the number of rotational inconsistencies, the exact number of shifts required has been calculated as the maximum angular deviation of two images of

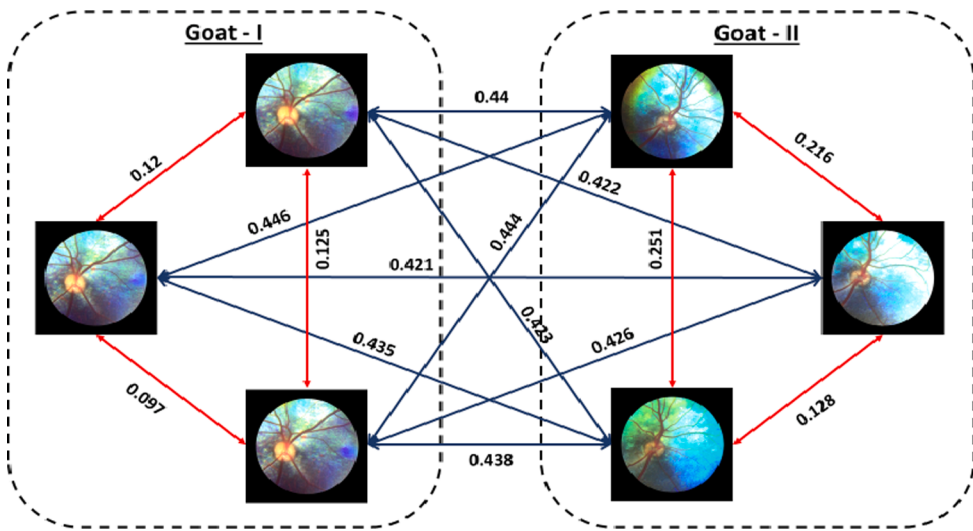


Fig. 12. Matching Perspective for “RetIS”.

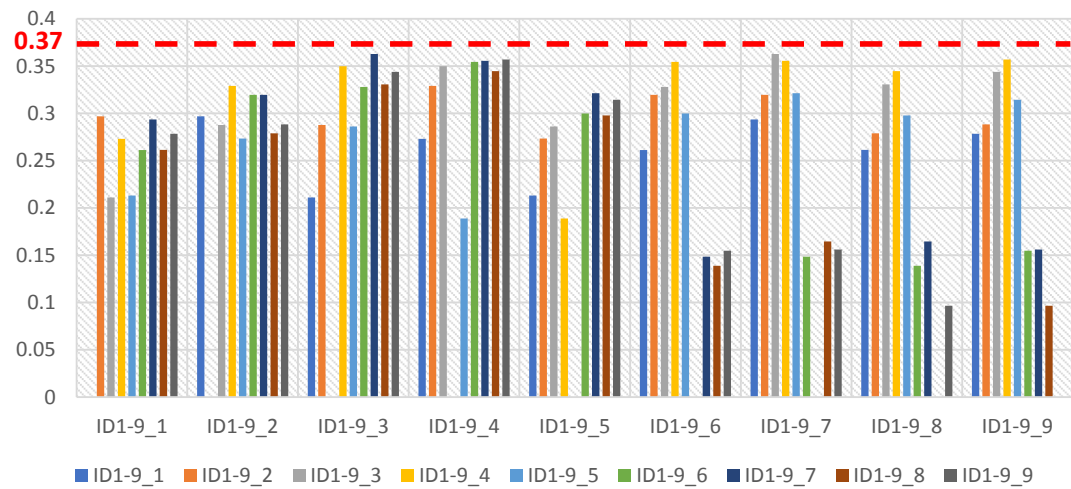


Fig. 13. Graph for hamming distance between same individual goat.

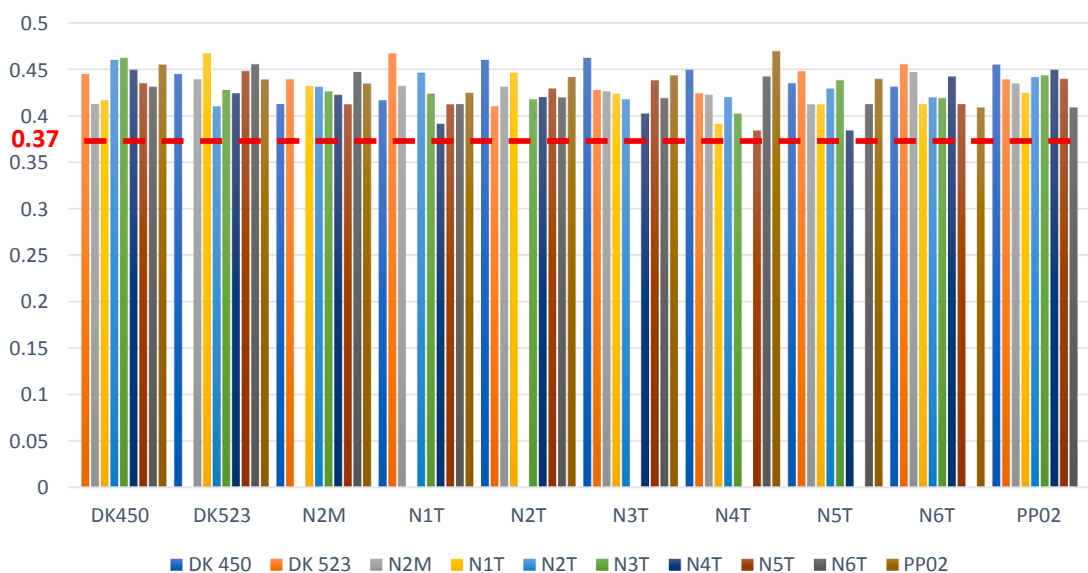


Fig. 14. Graph for hamming distance between different individual goat.

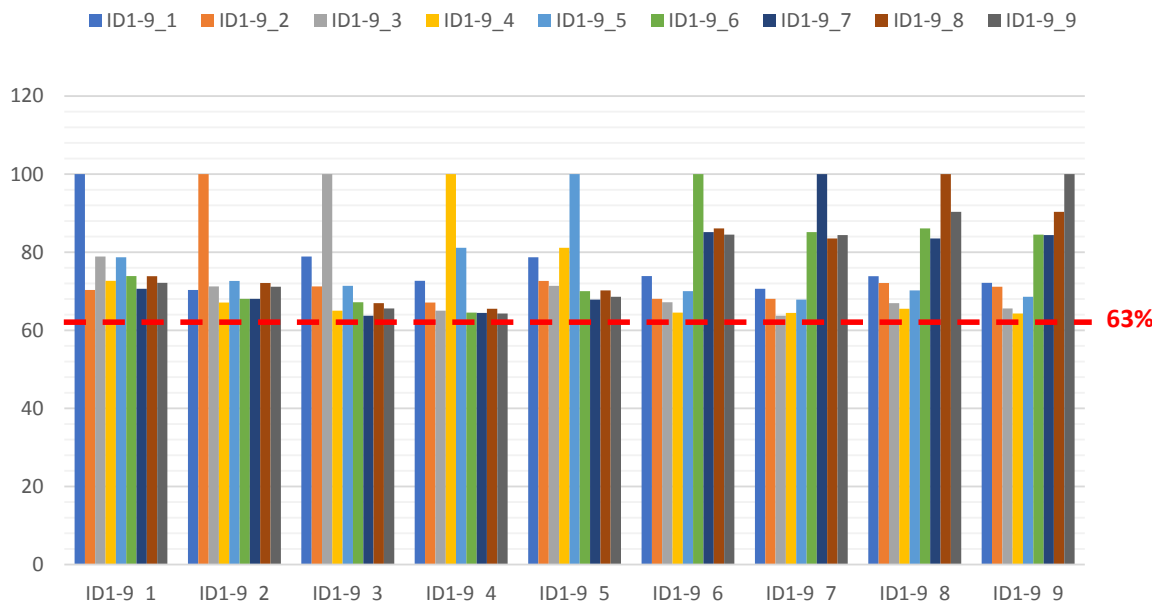


Fig. 15. Graph for Matching Percentage between same individual goat.

the same eye, one rotated in a direction opposite to that of the other (Fig. 11).

In this example, one filter has been used to perform encoding of the templates, so only two bits are moved at each shift. Theoretically, the lowest hamming distance (Atallah and Duket, 2011) 0.0 has been chosen as it corresponds to the best match between the templates. Also, a shift is explained as a shift left and right of the reference template. The outline of matching for “RetIS” is depicted in Fig. 12, where (—) indicates matching between templates of same goat images taken at different point of time and (—) indicates matching between templates for images of Goat I & Goat II. Each of 3 images of Goat I & II are performed with intra-class matching wherein the hamming distance is <0.37 and for inter-class matching, hamming distance comes out to be >0.37 .

4. Results & discussion

The template generated has been stored in the database and eventually used for matching between same and different goats. Hamming Distance (Atallah and Duket, 2011) and Matching Percentage

(interconversion is shown in Eq. (8)) have been used as parameters to find the threshold for matching and mismatching. One can see the change in values of hamming distance for the same goat retina taken at a different point of time. This is due to the change in the environment and the movement of the eye ball at every point of time. Considering this situation, a graph has been plotted (as shown in Fig. 13) between hamming distance and Goat ID.

Also, hamming distance between different individual goats have also been plotted and shown in Fig. 14, where a distinct 1:M matching (M is the number of Goats present in the database) is performed between a template for the retinal image of a particular Goat with all other templates of different goat images present in the database.

The change in the values of hamming distance as shown in Fig. 14 is primarily due to the change in the pattern of the retina for different goats. The change in the environment, movement of eye ball and others also affects the hamming distance but, never crosses the red dashed line mentioned in the graph. Similarly, for same goat individual, as shown in Fig. 13, the movement in the eyeball and other factors never let the matching values cross the red-dashed marker spotted in the figure itself.

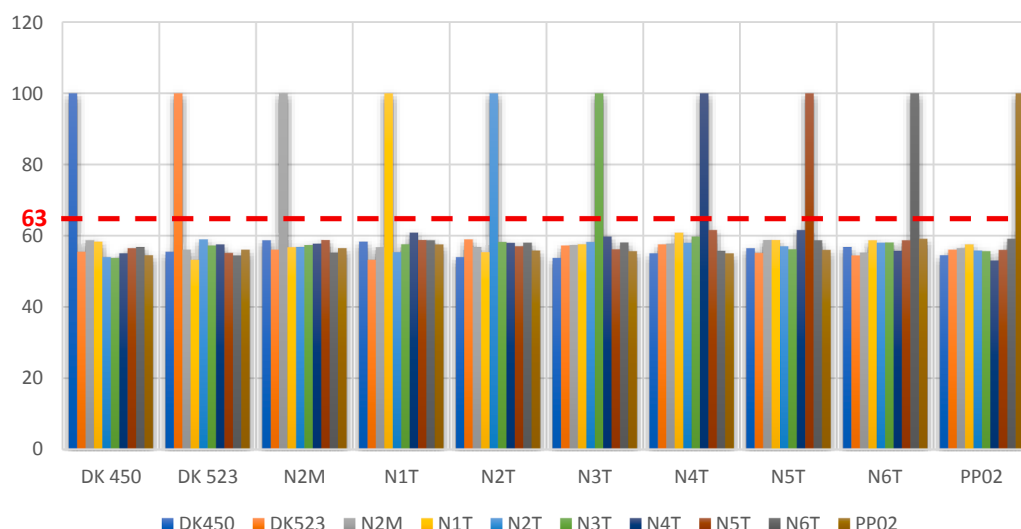


Fig. 16. Graph for Matching Percentage between Different individual goat.

Table 3

Hamming distances of same goat retina images of ID1-9_1 to ID1-9_9.

Goat ID	ID1-9_1	ID1-9_2	ID1-9_3	ID1-9_4	ID1-9_5	ID1-9_6	ID1-9_7	ID1-9_8	ID1-9_9
ID1-9_1	0	0.29684	0.2111	0.2731	0.2131	0.2612	0.2935	0.2613	0.2784
ID1-9_2		0	0.2877	0.329	0.2734	0.3195	0.3195	0.2789	0.2883
ID1-9_3			0	0.3498	0.2862	0.328	0.3628	0.3306	0.3439
ID1-9_4				0	0.1888	0.3545	0.3555	0.3447	0.3569
ID1-9_5					0	0.2999	0.3213	0.2978	0.3143
ID1-9_6						0	0.1484	0.1389	0.1548
ID1-9_7							0	0.1646	0.156
ID1-9_8								0	0.0965
ID1-9_9									0

Table 4

Matching percentage of same goat retina images of ID1-9_1 to ID1-9_9.

Goat ID	ID1-9_1	ID1-9_2	ID1-9_3	ID1-9_4	ID1-9_5	ID1-9_6	ID1-9_7	ID1-9_8	ID1-9_9
ID1-9_1	100	70.316	78.89	72.69	78.69	73.88	70.65	73.87	72.16
ID1-9_2		100	71.23	67.10	72.66	68.05	68.05	72.11	71.17
ID1-9_3			100	65.02	71.38	67.20	63.72	66.94	65.61
ID1-9_4				100	81.12	64.55	64.45	65.53	64.31
ID1-9_5					100	70.01	67.87	70.22	68.57
ID1-9_6						100	85.16	86.11	84.52
ID1-9_7							100	83.54	84.40
ID1-9_8								100	90.35
ID1-9_9									100

After performing the matching and mismatching between all combinations of images of goat present in the database, the authors inferred to the consideration of the red dashed line as the point of maximal mismatching and minimal matching. This line can be considered as a

Table 5

Matching percentages of three different images from each individual goat.

Goat ID	ID 1	ID 2	ID 3	BEST PIC
DK450	100	88.21	88.89	DK450_170
DK523	100	83.46	70.80	DK523_269
N2M	100	70.64	74.20	N2M-350
N1T	100	82.52	70.01	N1T-092
N2T	100	74.53	79.61	N2T-576
N3T	100	70.1	72.5	N3T-027
N4T	100	79.51	81.36	N4T-877
N5T	100	72.47	69.81	N5T_553
N6T	100	68.97	67.41	N6T_533
PP02	100	72.34	74.25	PP02_621

The “BEST PIC” column indicates the image satisfying nearly all the quality of the defined image acquisition standards for “RetIS” (Refer Section 4.2).

threshold having value as 0.37, where hamming distance of same goat would lie between 0 and 0.37 and that of different goat images would have values greater than 0.37.

The conversion between matching percentage and hamming distance can be perceived from Eq. (8) and similar graph having same and different goat images, considering Matching Percentage as the parameter is depicted in Fig. 15 & Fig. 16 respectively.

$$\text{Matching Percentage} = (1 - \text{Hamming Distance}) * 100\% \quad (8)$$

From Eq. (8), the threshold of 0.37 can be interconverted to a matching of 63%, where same goats would have matching more than 63% & different goats would have matching less than 63%.

4.1. Same individual goat

The following Table 3 shows the hamming distance of 9 images of a particular goat, taken at different point of time. The difference in the environment, movement in the eyeball created variations in the images

Table 6

Hamming distance of different goat retina images.

	DK 450	DK 523	N2M	N1T	N2T	N3T	N4T	N5T	N6T	PP02
DK450	0	0.445	0.4128	0.4167	0.4602	0.4624	0.4496	0.435	0.4314	0.4551
DK523		0	0.4393	0.4674	0.4102	0.4277	0.4243	0.4482	0.4556	0.4392
N2M			0	0.4321	0.4313	0.4263	0.4225	0.4122	0.4473	0.4348
N1T				0	0.4465	0.4238	0.3913	0.4122	0.4126	0.4247
N2T					0	0.4177	0.4201	0.4294	0.4198	0.4417
N3T						0	0.4025	0.4383	0.4191	0.4434
N4T							0	0.3842	0.4423	0.4696
N5T								0	0.4126	0.4398
N6T									0	0.4089
PP02										0

Table 7

Matching percentage of templates for different goat retina images.

	DK 450	DK 523	N2M	N1T	N2T	N3T	N4T	N5T	N6T	PP02
DK450	100	55.5	58.72	58.33	53.98	53.76	55.04	56.5	56.86	54.49
DK523		100	56.07	53.26	58.98	57.23	57.57	55.18	54.44	56.08
N2M			100	56.79	56.87	57.37	57.75	58.78	55.27	56.52
N1T				100	55.35	57.62	60.87	58.78	58.74	57.53
N2T					100	58.23	57.99	57.06	58.02	55.83
N3T						100	59.75	56.17	58.09	55.66
N4T							100	61.58	55.77	53.04
N5T								100	58.74	56.02
N6T									100	59.11
PP02										100

of the retina, but none of them crossed the threshold on 0.37, as claimed. The value in the highlighted cell means the hamming distance between the templates of retina images for Goat ID: ID1-9_3 vs. ID1-9_5, being less than 0.37.

The values depicted in Table 3 are converted to a matching percentage following Eq. (8) and are shown in Table 4. The highlighted cell indicates a matching of 71.38% between ID1-9_3 vs. ID1-9_5, which proves that the templates of the images are from same goat retina.

The graphical representation of Table 4 is shown in Fig. 15 for the matching among the IDs of same goats consisting of pictures taken at different point of time, the matching percentage being more than 63% for all the cases.

The following table (Table 5), shows matching percentages among the templates of three images of each goat taken at different point of time for ten different goats. Intra-class matching has been performed and respective percentages has been given in Table 5.

4.2. Different individual goat

The following Table 6 shows the hamming distance of goats between the inter-class BEST_PIC images from Table 5, to get the maximum mismatch. It has been observed that the mismatch is above the described threshold (0.37 being the minimum mismatch), thus proving its solidarity. The value in the highlighted cell means the hamming distance between the templates of retina images for Goat ID: N2T vs. N3T. ‘0’ indicates matching between same retina image.

The values depicted in Table 6 are converted to a matching percentage following Eq. (8) and are shown in Table 7. The highlighted cell indicates a matching of 58.23% between N2T vs.N3T, which proves the goats as different. ‘100’ indicates matching between templates of same retina image.

The graphical representation of Table 7 is shown in Fig. 16 for the IDs of different goats, matching percentage being less than 63% for all cases except between the same identical images showing a matching

Table 8
Performance evaluation of “RetIS”.

Category	Characteristics
True Positive (TP)	Matching Score < Matching Score Threshold Actual Goat ID = Calculated Goat ID
False Positive (FP)	Matching Score < Matching Score Threshold Actual Goat ID ≠ Calculated Goat ID
False Negative (FN)	Matching Score > Matching Score Threshold

percentage of 100%.

5. Performance evaluation of “RetIS”

The performance characteristics of the proposed algorithm has been classified in Table 8, having the metrics of True Positive, False Positive and False Negative depending on which Precision, Recall and Accuracy have thus been calculated.

Based on the TP, FP & FN values, important metrics regarding performance evaluation of “RetIS” can be calculated.

(i) **Precision:** It defines the no. of images that are actually true out of all the images that the algorithm, “RetIS” claim to be true.

$$\text{Precision} = \frac{\text{TP}}{\text{TP} + \text{FP}}$$

(ii) **Recall:** It defines the number of images that the algorithm claim to be true out of all the images in the dataset.

$$\text{Recall} = \frac{\text{TP}}{\text{TP} + \text{FN}}$$

(iii) **Accuracy:** It defines the number of claims by “RetIS”, based on calculations to be true out of all calculations by the algorithm.

$$\text{Accuracy} = \frac{\text{TP}}{\text{TP} + \text{FP} + \text{FN}}$$

An algorithm is said to be perfect if it is able to claim exact result based on the threshold in all the images correctly. For example, if there are ‘y’ images, for an algorithm to be perfect, TP = y, FP = 0, FN = 0. Thus, Precision = 100%, Recall = 100% & Accuracy = 100%. To build a perfect algorithm, the main aim should be to reduce FP & FN and

Table 9
Performance analysis for the algorithm “RetIS”.

	Total Number	Accuracy	Recall	Precision
True Positive (TP)	198	$\frac{TP}{TP + FN + FP}$	$\frac{TP}{TP + FN}$	$\frac{TP}{TP + FP}$
False Positive (FP)	0	$\frac{0}{198}$	$\frac{0}{198}$	$\frac{0}{198}$
False Negative (FN)	2	$\frac{198 + 2 + 0}{198}$ 0.99 or 99%	$\frac{198 + 2}{198}$ 0.99 or 99%	$\frac{198 + 0}{198 + 0}$ 1 or 100%

increase TP, such that the values of Precision, Recall & Accuracy reach close to 100%.

For “RetIS”, total goats taken into experimentation is 12 and an average of 17 fundus images of each goats (Fixing to the retina of left eye only universally for “RetIS” technology) have been captured in an

uncontrolled environment following the defined image acquisition standards (Table 1 and Fig. 3) of “RetIS” wherein each of 17 retinal images for respective individuals have been acquired after a specific interval of time, which also resulted in the change in the immediate environment, and due to which the intra-class matching percentage never came out to be same but always above the threshold level proving the credibility of the technology. The analysis of Precision, Recall and Accuracy have been shown in Table 9 and referring the definition of terms from Table 8:

6. Performance Comparison of “RetIS”

The algorithm of “RetIS” has been compared with different techniques and technologies to that of identifying different animals and is summarised in Table 10.

Table 10

Comparison with other technologies for identification. (See below-mentioned references for further information.)

Literature Cited	Methodology	Metric	No. of Images	Capturing Conditions	Accuracy or Recognition Rate
(Lu et al., 2014)	Iris Acquisition, fitting inner & outer boundaries as two ellipses in segmentation, normalization, encoding & matching	Cow Iris	60 Iris Images from 6 Eyes	Not Mentioned	98.33%
(Rusk et al., 2006)	Descriptive Statistics, Analysis of Variance to compare between species and locations	Sheep Retina	220 Sheep Fundus Images	Not Mentioned	72.4%
(Jarraya et al., 2016)	Horses' face recognition; frontal face; Gabor features; LBP features;	Horse Facial Texture	329 Face Images for Training and 141	Controlled	95.74%
	Euclidean distance, mahcosine distance		Images for Test		
(De & Ghoshal, 2016)	Goat Iris pattern deviation from standard circular shaped	Structural	700 iris images	Controlled (illumination)	97.85%
(Goat Iris)	Mean, Variance, Skewness, Kurtosis	Statistical	-do-	-do-	91.82%
	2D Fourier Transform	Spectral	-do-	-do-	89.10%
Our Paper	CLAHE, Circular Segmentation, Normalization, Log-Gabor Wavelet, Hamming Distance	Retinal Imaging	200 Fundus Images	Uncontrolled	99%

7. “GoatRetDB-KGEC” database

A database has been created consisting of the retinal images of goats captured from the farm of Indian Veterinary Research Institute, ERS Kalyani, West Bengal, India. The database holds at an average of 17 fundus images from the left eye for each of 13 different goats and thereby used for application and validation of the technology of “**RetIS**”. The images have been captured following the image acquisition standards and selection standards of “**RetIS**” and have been graded based on the quality, clarity and coverage of the retina maximising the display. From Table 5, it can be perceived that three different IDs have been created where ID1 corresponds to the exactly same image used for matching. Due to this, the matching percentage always results in 100%. ID2 and ID3 depicts the two most qualified images out of which one can be considered as the “**BEST_PIC**” and hence listed in the **BEST_PIC** column. The maximum coverage of the retina with optic disc fitting nearly the centre of the screen with high clarity in the image qualifies the criteria for high quality images. These images help in identifying the maximal mismatching in case of inter-class matching. On the other hand, the lowest quality image just fitting the quality for selection standards for “**RetIS**” helps in finding the minimal matching in case of intra-class matching problem. Hence, performance has a direct link in establishing the efficacy of the technology by analysing the image characteristics of the images thus used.

8. Conclusion

In this paper, a novel unique identification technology has been devised and proposed in identifying & recognizing individual goat through retinal image analysis. The threshold value has been calculated as 0.37 or 63% for matching & mismatching between same and different goats respectively. Comparing with other technologies of animal identification, “**RetIS**” has been found as the most accurate (*Accuracy 99%*) and precise (*Precision 100%*) in identifying & recognizing the goats against all odds of heterogenous colour intensity of the background and arbitrary size of blood vessels. This technology has been able to generate a tamper-proof, unique & reliable identification to goats to prevent any sort of illegal activities. Also, a database for each individual can be maintained soon after weaning to keep track of all the morphological information and vaccination measures from birth till death for the traceability of the safe chevon production system in the meat processing industry.

CRediT authorship contribution statement

Subhranil Mustafi: Writing - original draft, Methodology, Conceptualization, Visualization, Investigation, Formal analysis. **Pritam Ghosh:** Writing - review & editing, Visualization, Investigation, Formal analysis. **Satyendra Nath Mandal:** Conceptualization, Resources, Supervision, Project administration.

Declaration of Competing Interest

The authors declare that they have no known competing financial interests or personal relationships that could have appeared to influence the work reported in this paper.

Acknowledgement

The authors would like to express sincere gratitude to Digital India Corporation (formerly Medialab Asia) to grant us this research work under the project “ImageIDGP” under ITRA-Ag&Food, Dr. Amitabha Bandyopadhyay, Senior Consultant, ITRA-Ag&Food for suggesting us with new turnabouts in developing “**RetIS**” algorithm, Sanket Dan, Rajiv Gandhi National Fellow, Subhajit Roy, Lecturer, Gangarampur Govt. Polytechnic, West Bengal, Kaushik Mukherjee, Lecturer, Kalyani

Government Engineering College, Kunal Roy, Junior Research Fellow (WBDSTBT), Dr. Dilip Kumar Hajra, Assistant Professor, Uttar Banga Krishi Viswavidyalaya, Dr. Shyamal Naskar, Principal Scientist, IVRI, ERS-Kalyani, Dr. Santanu Banik, Principal Scientist, ICAR, NRC on Pig, Rani, Guwahati, Assam and Dr. Saurabh Kumar Das, Principal of Kalyani Government Engineering College for helping us to carry out this research work.

References

- Atallah, M.J., Duket, T.W., 2011. Pattern matching in the Hamming distance with thresholds. *Inform. Process. Lett.* 111 (14), 674–677. <https://doi.org/10.1016/j.ipl.2011.04.004>.
- Atropine Sulfate Drops, n.d. <https://www.webmd.com/drugs/2/drug-156298/atropine-sulfate-pf-ophthalmic-eye/details>.
- Bernardes, R., Serrano, P., Lobo, C., 2011. Digital ocular fundus imaging: a review. *Ophthalmologica* 226 (4), 161–181. <https://doi.org/10.1159/000329597>.
- Bevilacqua, V., Cariello, L., Columbo, D., Daleno, D., Fabiano, M.D., Giannini, M., Mastronardi, G., Castellano, M., 2008. Retinal fundus biometric analysis for personal identifications. *Lecture Notes in Computer Science (Including Subseries Lecture Notes in Artificial Intelligence and Lecture Notes in Bioinformatics)*, 5227 LNAI, 1229–1237. https://doi.org/10.1007/978-3-540-85984-0_147.
- Bhayani, D.M., Vyas, Y.L., 2014. Veterinary Science Histomorphological and Micrometrical Study of the Retina in Adult Rakesh Kumar Barhaiya Malsawmkima Department of Veterinary Anatomy and Histology, College of Veterinary Science & A. H. Anand Agricultural University, Anand Department. 11, 100–102.
- Chawla, S.K., Oberoi, A., 2011. A robust algorithm for iris segmentation and normalization using Hough transform. *Global J. Bus. Manage. Inform. Technol.*, November.
- Chihaoui, T., Jlassi, H., Kachouri, R., Hamrouni, K., Akil, M., 2016. Personal verification system based on retina and SURF descriptors. In: 13th International Multi-Conference on Systems, Signals and Devices, SSD 2016, 280–286. <https://doi.org/10.1109/SSD.2016.7473709>.
- Chihaoui, T., Kachouri, R., Jlassi, H., Akil, M., Hamrouni, K., 2015. Human identification system based on the detection of Optical Disc Ring in retinal images. In: 5th International Conference on Image Processing, Theory, Tools and Applications 2015, IPTA 2015, 263–267. <https://doi.org/10.1109/IPTA.2015.7367143>.
- De Luis-García, R., Alberola-López, C., Aghzout, O., Ruiz-Alzola, J., 2003. Biometric identification systems. *Signal Process.* 83 (12), 2539–2557. <https://doi.org/10.1016/j.sigpro.2003.08.001>.
- De, P., Ghoshal, D., 2016. Recognition of non circular iris pattern of the goat by structural, statistical and Fourier descriptors. *Procedia Comput. Sci.* 89, 845–849. <https://doi.org/10.1016/j.procs.2016.06.070>.
- Deljavan Amiri, M., Akhlaqian Tab, F., Barkhoda, W., 2009. Retina identification based on the pattern of blood vessels using angular and radial partitioning. *Lecture Notes in Computer Science (Including Subseries Lecture Notes in Artificial Intelligence and Lecture Notes in Bioinformatics)*, 5807 LNCS, 732–739. https://doi.org/10.1007/978-3-642-04697-1_68.
- Elangovan, P., Nath, M.K., 2019. A review: person identification using retinal fundus images. *Int. J. Electron. Telecommun.* 65 (4), 585–596. <https://doi.org/10.24425/ijet.2019.129817>.
- Fraz, M.M., Remagnino, P., Hoppe, A., Uyyanavar, B., Rudnicka, A.R., Owen, C.G., Barman, S.A., 2012. Blood vessel segmentation methodologies in retinal images - a survey. *Comput. Methods Programs Biomed.* 108 (1), 407–433. <https://doi.org/10.1016/j.cmpb.2012.03.009>.
- Fukuta, K., Nakagawa, T., Hayashi, Y., Hatanaka, Y., Hara, T., Fujita, H., 2008. Personal identification based on blood vessels of retinal fundus images. *Medical Imaging 2008: Image Process.* 6914, 69141V. <https://doi.org/10.1117/12.769330>.
- Gonzales Barron, U., Corkery, G., Barry, B., Butler, F., McDonnell, K., Ward, S., 2008. Assessment of retinal recognition technology as a biometric method for sheep identification. *Comput. Electron. Agric.* 60 (2), 156–166. <https://doi.org/10.1016/j.compag.2007.07.010>.
- Jarraya, I., Ouarda, W., Alimi, A.M., 2016. A preliminary investigation on horses recognition using facial texture features. In: Proceedings - 2015 IEEE International Conference on Systems, Man, and Cybernetics, SMC 2015, 1, 2803–2808. <https://doi.org/10.1109/SMC.2015.489>.
- Johar, T., Kaushik, P., 2015. Iris Segmentation and Normalization using Daugman's Rubber Sheet Model. *Int. J. Scientific Technical Adv.* 1 (1), 11–14. http://www.ijsta.com/papers/ijstav1n1/IJSTA_V1N1P3_PP11-14.pdf.
- Kachouri, R., Akil, M., Elloumi, Y., 2020. Retinal Image Processing in Biometrics. In: Nait-ali, A. (Ed.), *Hidden Biometrics: When Biometric Security Meets Biomedical Engineering*. Springer Singapore, pp. 167–184. https://doi.org/10.1007/978-981-13-0956-4_10.
- Kane, E., 2011. Iris scan technology for horses. 2001, 4–7.
- Köse, C., Ikbabs, C., 2011. A personal identification system using retinal vasculature in retinal fundus images. *Expert Syst. Appl.* 38 (11), 13670–13681. <https://doi.org/10.1016/j.eswa.2011.04.141>.
- Liu, C., Sui, X., Liu, Y., Kuang, X., Gu, G., Chen, Q., 2019. Adaptive contrast enhancement based on histogram modification framework. *J. Mod. Opt.* 66 (15), 1590–1601. <https://doi.org/10.1080/09500340.2019.1649482>.
- Lu, Y., He, X., Wen, Y., Wang, P.S.P., 2014. A new cow identification system based on iris analysis and recognition. *Int. J. Biometrics* 6 (1), 18–32. <https://doi.org/10.1504/IJBM.2014.059639>.

- Maltoni, Davide, Maio, Dario, Jain, Anil K., Prabhakar, S., 2009. Handbook of Fingerprint Recognition. Springer-Verlag London. <https://doi.org/10.1007/978-1-84882-254-2>.
- Muhammed, Lamia AbedNoor, 2018. Localizing optic disc in retinal image automatically with entropy based algorithm. *Int. J. Biomed. Imaging* 2018, 1–7. <https://doi.org/10.1155/2018/2815163>.
- Mustafi, S., Ghosh, P., Dan, S., Mukherjee, K., Roy, K., Mandal, S.N., 2020. In: Mallick, P. K., Meher, P., Majumder, A., Das, S.K. (Eds.), Electronic Systems and Intelligent Computing. Lecture Notes in Electrical Engineering, 686. Springer, Singapore. https://doi.org/10.1007/978-981-15-7031-5_7.
- Mustafi, S., Ghosh, P., Dan, S., Mukherjee, K., Roy, K., Mandal, S.N., 2021. Entrepreneurship possibility on goat farming in India. *Acta Scientific Agric.* 5 (2), 24–32. <https://www.actascientific.com/ASAG/ASAG-05-0944.php>.
- Nava, R., Escalante-Ramírez, B., Cristóbal, G., 2012. Texture image retrieval based on log-gabor features. In: Alvarez, L., Mejail, M., Gomez, L., Jacobo, J. (Eds.), *Progress in Pattern Recognition, Image Analysis, Computer Vision, and Applications*. Springer, Berlin Heidelberg, pp. 414–421.
- M. Ortega, C.Marino, M.G. Penedo, M. Blanco, F.G. A., 2006. Biometric authentication using digital retinal images. In: Proceedings of the 5th WSEAS International Conference on Applied Computer Science, Hangzhou, China, pp. 422–427. <https://citeeseerx.ist.psu.edu/viewdoc/download?doi=10.1.1.534.2322&rep=rep1&type=pdf>.
- Pradeep Kumar, P.I.K.R., 2014. Log gabor filter based feature detection in image verification application. *Int. J. Sci. Res. (IJSR)* 3(12), 703–707. <https://www.ijsr.net/archive/v3i12/U1VCMTQ0Nzk=.pdf>.
- Panwar, N., Huang, P., Lee, J., Keane, P.A., Chuan, T.S., Richhariya, A., Teoh, S., Lim, T. H., Agrawal, R., 2016. Fundus photography in the 21st century - a review of recent technological advances and their implications for worldwide healthcare. *Telemed. E-Health* 22 (3), 198–208. <https://doi.org/10.1089/tmj.2015.0068>.
- Rani, B.M.S., Rani, A.J., 2017. A survey on classification techniques in biometric retinal system. In: *IEEE International Conference on Innovations in Green Energy and Healthcare Technologies - 2017, IGEHT 2017*, 1–7. <https://doi.org/10.1109/IGEHT.2017.8094065>.
- Roy, S., Dan, S., Mukherjee, K., Nath Mandal, S., Hajra, D.K., Banik, S., Naskar, S., 2021. Black Bengal Goat Identification Using Iris Images. In: Bhattacharjee, D., Kole, D.K., Dey, N., Basu, S., Plewczynski, D. (Eds.), *Proceedings of International Conference on Frontiers in Computing and Systems*. Springer Singapore, pp. 213–224.
- Rubini, C., Pavithra, N., 2019. Contrast Enhancement of MRI Images using AHE and CLAHE Techniques. *Int. J. Innovative Technol. Exploring Eng.* 9 (2), 2442–2445. <https://doi.org/10.35940/ijitee.b7017.129219>.
- Rusk, C.P., Blomeke, C.R., Balschweid, M.A., Elliott, S.J., Baker, D., 2006. An evaluation of retinal imaging technology for 4-H beef and sheep identification. *J. Extension* 44 (5), 1–14.
- S.L., S.J., S, D.S.K., 2017. Beef cattle identification using PCA and other cattle. *Int. J. Eng. Sci. Res. Technol.* 6(11), 177–185.
- Setiawan, A.W., Mengko, T.R., Santoso, O.S., Suksmono, A.B., 2013. Color retinal image enhancement using CLAHE. In: *Proceedings - International Conference on ICT for Smart Society 2013: "Think Ecosystem Act Convergence"*, ICSS 2013, 215–217. <https://doi.org/10.1109/ICTSS.2013.6588092>.
- Shayduk, N.K., Cleland, T., 2016. Biometric identification via retina scanning with liveness detection using speckle contrast imaging. In: *Proceedings - International Carnahan Conference on Security Technology*, 0. <https://doi.org/10.1109/CCST.2016.7815706>.
- Singh, A., Dutta, M.K., Sharma, D.K., 2016. Unique identification code for medical fundus images using blood vessel pattern for tele-ophthalmology applications. *Comput. Methods Programs Biomed.* 135, 61–75. <https://doi.org/10.1016/j.cmpb.2016.07.011>.
- Small, R.W., 2015. Review of Livestock Identification and Traceability in the UK. Defra Research Contract GC0146 Development of Co-Ordinated in Situ and Ex Situ UK Farm Animal Genetic Resources Conservation Strategy and Implementation Guidance, 1–61. <https://www.gov.uk/cattle-identification-registration-and-movement>.
- The Finest Ophthalmic Imaging catalog, 2019. <https://volk.com/cleaning-and-care>.
- Tower, P., 1955. The fundus oculi in monozygotic twins. *A.M.A. Arch. Ophthalmol.* 54 (2), 225. <https://doi.org/10.1001/archoph.1955.00930020231010>.
- Unar, J.A., Seng, W.C., Abbasi, A., 2014. A review of biometric technology along with trends and prospects. *Pattern Recogn.* 47 (8), 2673–2688. <https://doi.org/10.1016/j.patcog.2014.01.016>.
- USER ' S MANUAL/INSTRUCTIONS FOR USE Volk iNview Retinal Camera. (n.d.).
- Zhi, Z., Cepurna, W.O., Johnson, E.C., Morrison, J.C., Wang, R.K., 2012. Impact of intraocular pressure on changes of blood flow in the retina, choroid, and optic nerve head in rats investigated by optical microangiography. *Biomed. Opt. Express* 3 (9), 2220. <https://doi.org/10.1364/boe.3.002220>.
- Zhu, Y., Tan, T., Wang, Y., 2000. Biometric personal identification based on iris patterns. In: *Proceedings - International Conference on Pattern Recognition*, vol. 15(2), pp. 801–804. <https://doi.org/10.12928/jti.v2i1.7-14>.